Animal Microbiome

RESEARCH

Open Access

Novel complete methanogenic pathways in longitudinal genomic study of monogastric age-associated archaea

Brandi Feehan[1], Qinghong Ran[1], Victoria Dorman[1], Kourtney Rumback[1], Sophia Pogranichniy[1], Kaitlyn Ward[1], Robert Goodband[2], Megan C. Niederwerder[3] and Sonny T. M. Lee[1*]

Abstract

Background Archaea perform critical roles in the microbiome system, including utilizing hydrogen to allow for enhanced microbiome member growth and influencing overall host health. With the majority of microbiome research focusing on bacteria, the functions of archaea are largely still under investigation. Understanding methanogenic functions during the host lifetime will add to the limited knowledge on archaeal influence on gut and host health. In our study, we determined lifelong archaea dynamics, including detection and methanogenic functions, while assessing global, temporal and host distribution of our novel archaeal metagenome-assembled genomes (MAGs). We followed 7 monogastric swine throughout their life, from birth to adult (1–156 days of age), and collected feces at 22 time points. The samples underwent gDNA extraction, Illumina sequencing, bioinformatic quality and assembly processes, MAG taxonomic assignment and functional annotation. MAGs were utilized in downstream phylogenetic analysis for global, temporal and host distribution in addition to methanogenic functional potential determination.

Results We generated 1130 non-redundant MAGs, representing 588 unique taxa at the species level, with 8 classified as methanogenic archaea. The taxonomic classifications were as follows: orders *Methanomassiliicoccales* (5) and *Methanobacteriales* (3); genera *UBA71* (3), *Methanomethylophilus* (1), *MX-02* (1), and *Methanobrevibacter* (3). We recovered the first US swine *Methanobrevibacter UBA71 sp006954425* and *Methanobrevibacter gottschalkii* MAGs. The *Methanobacteriales* MAGs were identified primarily during the young, preweaned host whereas *Methanomassiliicoccales* primarily in the adult host. Moreover, we identified our methanogens in metagenomic sequences from Chinese swine, US adult humans, Mexican adult humans, Swedish adult humans, and paleontological humans, indicating that methanogens span different hosts, geography and time. We determined complete metabolic pathways for all three methanogenic pathways: hydrogenotrophic, methylotrophic, and acetoclastic. This study provided the first evidence of acetoclastic methanogenesis in archaea of monogastric hosts which indicated a previously unknown capability for acetate utilization in methanogenesis for monogastric methanogens. Overall, we hypothesized that the age-associated detection patterns were due to differential substrate availability via the host diet and microbial metabolism, and that these methanogenic functions are likely crucial to methanogens across hosts. This study provided a comprehensive, genome-centric investigation of monogastric-associated methanogens which will further improve our understanding of microbiome development and functions.

*Correspondence:
Sonny T. M. Lee
leet1@ksu.edu
Full list of author information is available at the end of the article

Keywords Archaea, Methanogenesis, Microbiome, Swine, Monogastric

Introduction

The gastrointestinal system contains countless microorganisms spanning multiple kingdoms performing diverse functions. Archaea, bacteria, viruses, and fungi work in concert and competition to acquire nutrients and space [1]. The focus of previous gut microbiome research has predominantly been on the identification and function of bacteria [2, 3]. However, archaea have been demonstrated to be equally important members of the gastrointestinal microbiome [4]. Methanogenic archaea, or archaea which carry out methanogenesis, perform crucial roles in the gut [4, 5]. Yet, current research has not indicated how methanogenic gut functions change throughout the lifetime of monogastric hosts [6, 7]. With limited research on archaea, and even more minimal analysis on methanogenic functions, we are lacking an in-depth understanding of gastrointestinal associated methanogens, especially our comprehension of methanogen influence on gut and host health throughout host stages of life. By investigating monogastric associated methanogens with a longitudinal approach, we are adding essential knowledge to the limited understanding of monogastric methanogens.

While some beneficial and detrimental associations of archaea to host health have been reported, overall the role of archaea in health and disease is still under investigation [5]. To date, archaea have been associated with a few illnesses, primarily gastrointestinal disorders such as constipation [5, 8, 9] and obesity [5, 10]. Conversely, archaea have also been associated with beneficial attributes. For example, archaea metabolize trimethylamine (TMA), which is thought to decrease cardiovascular disease [4, 5]. This research has prompted further evaluation of archaea members as a probiotic for cardiovascular health [5, 11]. Moreover, archaea allow continued microbial metabolism, growth and action by lowering hydrogen gut levels [5]. Archaea's role of hydrogen utilization is especially important in the gut where microorganisms work in concert within the shared gut-microbiome system. However, with limited prior research, there is a critical need to understand the role of gastrointestinal archaea in health and sickness via hydrogen metabolism.

Overall, archaea are classified into four superphyla: *Euryarchaeota*, *Asgard*, *TACK* (*Thaumarchaeota*, *Aigarchaeota*, *Crenarchaeota* and *Korarchaeota*), and *DPANN* (*Diapherotrites*, *Parvarchaeota*, *Aenigmarchaeota*, *Nanoarchaeota*, and *Nanohaloarchaeota*) [12]. To date, *Asgard* archaea have not been indicated as methanogens [12], and *TACK* and *DPANN* have only been identified in non-host associated environmental sites [12–14]. Therefore, currently known host-associated gut methanogens fall within the seven orders of *Euryarchaeota*: *Methanobacteriales, Methanococcales, Methanomicrobiales, Methanosarcinales, Methanocellales, Methanopyrales, Methanomassiliicoccales* [15–18]. These *Euryarchaeota* orders are obligate anaerobes which perform methanogenesis to conserve energy for ATP production, where methane is a byproduct [15, 19]. Actions immediately following methanogenesis generate an ion gradient which is coupled with ATP production [20, 21].

Given the necessity for ATP production, it is unsurprising that historically, studies have primarily relied on the methanogenic gene methyl-coenzyme M reductase A (*mcrA*) or 16S rRNA for identification of gut-associated methanogens [7, 22–24]. *McrA* has been identified in all methanogens to date, as the protein performs a critical role in the final methane production step of methanogenesis [24, 25]. While prior research was heavily reliant on targeted PCR methodologies, we are in-large missing gene centric methanogenic understanding, from complete genetic sequencing, of gut-associated methanogens [26]. Functional methanogen studies become even more profound when evaluated in a longitudinal approach, especially when following the same hosts. In doing so, we can determine lifetime gut methanogen dynamics and host implications. Currently, studies which evaluate longitudinal methanogen dynamics typically involve ruminant hosts, such as cows, sheep, goats, and deer [27]. At the time of publication, we could not find a longitudinal study of methanogen genomes (i.e. not marker studies such as 16S rRNA or *mcrA*) following the same monogastrics hosts throughout their lifetime, highlighting the crucial need for such metagenomic longitudinal evaluations [6, 7]. Without this knowledge, we cannot determine lifetime dynamics of archaea, and how their methanogenic function may be related to age-associated factors, such as diet and host development.

Host-associated archaeal methanogens have been linked to various conditions of health and disease. Most archaea-centric intestinal microbiome studies have been conducted on a single time point in the lifetime of the host. Using molecular and cultural approaches, intestinal archaea have been identified in many hosts, including: humans, swine, horses, rats, birds, fish, and kangaroos [28]. Overall, these analyses reported that the most common methanogens in the gut are members of the *Methanobacteriales* and *Methanomassiliicoccales*

orders [28]. However, little is known about the presence and distribution of archaea through the lifetime of the swine. There is also a lack of data on the functions of the archaea in the swine gut. Overall, this knowledge gap has hindered the identification of factors that influence the diversity, abundance, and functions of archaea in the swine. In this study, we evaluated methanogen abundance and functions of 7 monogastric swine hosts over their lifetime at 22 timepoints from birth through adulthood (ages 1–156 days). We recovered 8 methanogenic archaea metagenome-assembled genomes (MAGs) that exhibited differential colonization patterns in the host at different ages. While distribution of methanogens across multiple hosts has been previously demonstrated, we recovered the first US swine *Methanobrevibacter UBA71 sp006954425* and *Methanobrevibacter gottschalkii* MAGs [28]. Moreover, we attributed methanogenic functional potential to our age-associated archaea, and identified the first evidence of acetoclastic methanogenesis in monogastric-associated archaea, found in our *Methanomassiliicoccales* MAGs, indicating a previously unknown capability of monogastric methanogens to utilize acetate in energy acquisition. Alternatively, we attributed hydrogenotrophic methanogenesis, where carbon dioxide (CO_2) is utilized, in the *Methanobacteriales*. We surmised that the age-associated detection patterns were due to differential substrate availability, which was highly influenced by diet. Altogether, we provided a comprehensive, genome-centric investigation of monogastric-associated archaea to further our understanding of microbiome development and function.

Results and discussion

Taxonomic classification of gut metagenome-assembled genomes

To broadly sample gut-associated microorganisms of the swine host across different age-associated growth stages, we obtained ~ 5.8×10^9 paired-end reads from Illumina NovaSeq sequencing data of 112 swine fecal samples (Fig. 1 and Additional file 1: Table S3). After quality trimming, we generated ~ 5.2×10^9 paired-end reads. The resulting 3 co-assemblies contained ~ 9.4×10^6 contigs that described approximately ~ 3.6×10^{10} nucleotides and ~ 3.7×10^7 genes. Using a combination of automatic and manual binning strategies, with thresholds of > 70% complete and < 10% redundancy, resulted in 4,556 metagenome-assembled genomes (MAGs). We further removed redundancy by selecting a single representative for each set of genomes that shared an average nucleotide identity (ANI) of greater than 95%, resulting in 1,130 final non-redundant MAGs (nr-MAGs) (Additional file 1: Table S3). Among the nr-MAGs, we recovered an average of 203 ± 187 contigs, with an average N50 of 32,737 ± 35,205. The resolved nr-MAGs had completion values of 87.9% ± 8.6% and redundancy values of 3.2% ± 2.6%. The genomic lineages for archaeal and bacterial nr-MAGs based on domain-specific single-copy core genes resolved to 20 phyla (2 archaea phyla and 18 bacterial phyla) and 588 species (5 archaea species and 582 bacterial species). We could also assign 88.4% of the bacterial and archaeal nr-MAGs to their genera.

Resolved archaeal MAGs are genetically and phylogenetically similar to diverse hosts and geographic disbursed archaea

Among the 1,130 nr-MAGs that we resolved, our genomic collection also included 8 archaea nr-MAGs (hereafter known as archaea-MAGs; Ar-1 through Ar-8; Table 1; Additional file 1: Table S3). We observed that our resolved archaea-MAGs harbored genes which encoded for critical methyl-coenzyme M reductase (*mcrABG*) proteins required for methanogenesis, including *mcrA* which is typically utilized for methanogen classification [29, 30] (Additional files 1: Tables S3 and 2: Table S4). To our best knowledge, these MAGs represent the first

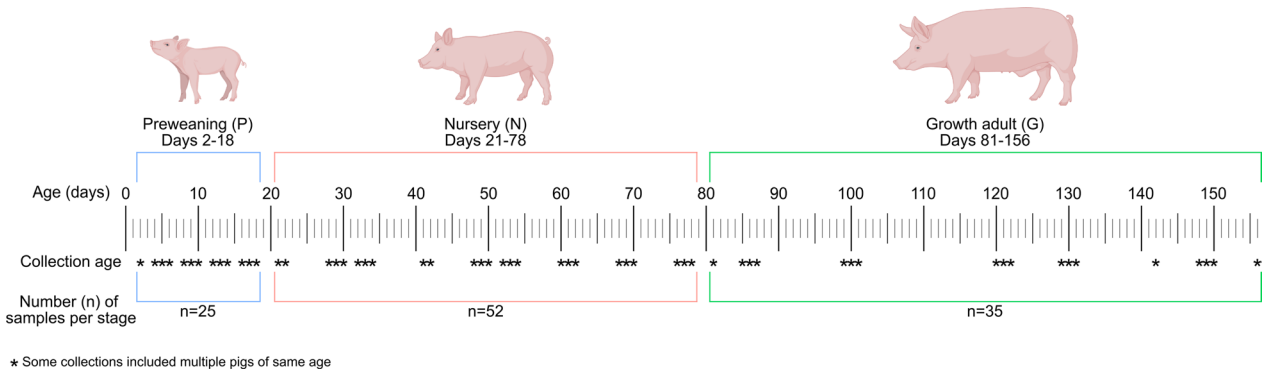

Fig. 1 Study schematics of 7 swine hosts including fecal sampling ages and developmental stages

Table 1 Anvi'o results, including taxonomic assignment, of 8 archaea-MAGs

MAG ID	Total length (nucleotides)	Number of contigs	N50	GC content (%)	Percent completion (%)	Percent redundancy (%)	Domain	Phylum	Class	Order	Family	Genus	Species
Ar-1	1,634,787	68	46,847	53	97	0	Archaea	*Thermoplasmatota*	*Thermoplasmata*	*Methanomassiliicoccales*	*Methanomethylophilaceae*	*UBA71*	*UBA71 sp006954425*
Ar-2	2,118,112	250	15,626	54	95	1	Archaea	*Thermoplasmatota*	*Thermoplasmata*	*Methanomassiliicoccales*	*Methanomethylophilaceae*	*UBA71*	*UBA71 sp006954425*
Ar-3	960,519	435	2,416	56	80	9	Archaea	*Thermoplasmatota*	*Thermoplasmata*	*Methanomassiliicoccales*	*Methanomethylophilaceae*	*UBA71*	*UBA71 sp006954425*
Ar-4	1,269,388	112	15,439	56	83	4	Archaea	*Thermoplasmatota*	*Thermoplasmata*	*Methanomassiliicoccales*	*Methanomethylophilaceae*	*Methanomethylophilus*	*Methanomethylophilus alvus*
Ar-5	957,172	18	59,251	32	72	0	Archaea	*Methanobacteriota*	*Methanobacteria*	*Methanobacteriales*	*Methanobacteriaceae*	*Methanobrevibacter*	*Methanobrevibacter smithii*
Ar-6	1,724,540	38	68,759	33	100	0	Archaea	*Methanobacteriota*	*Methanobacteria*	*Methanobacteriales*	*Methanobacteriaceae*	*Methanobrevibacter*	N/A
Ar-7	1,341,189	53	49,597	48	99	0	Archaea	*Thermoplasmatota*	*Thermoplasmata*	*Methanomassiliicoccales*	*Methanomethylophilaceae*	*MX-02*	*MX-02 sp006954405*
Ar-8	1,513,577	47	51,497	31	100	1	Archaea	*Methanobacteriota*	*Methanobacteria*	*Methanobacteriales*	*Methanobacteriaceae*	*Methanobrevibacter*	*Methanobrevibacter gottschalkii*

genomic evidence of putative methanogens differential colonization pattern of the monogastric gut. The resolved methanogen MAGs had an average genome size of 1.4 Mbp, 1,573 KEGG gene annotations, 1,535 COG gene annotations, and a GC content ranging from 31 to 56% (Table 1; Additional file 1: Table S3). We resolved 7 of the methanogen MAGs to the species level with one archaea-MAG resolving to the genus level (Table 1; Additional file 1: Table S3). Our resolved archaea-MAGs were assigned to the following orders: *Methanomassiliicoccales* (5) and *Methanobacteriales* (3). Moreover, the genera were as follows: *UBA71* (3), *Methanomethylophilus* (1), *MX-02* (1), and *Methanobrevibacter* (3).

We downloaded 95 *Methanomassiliicoccales* and 97 *Methanobacteriales* genomes to investigate the phylogenetic relationship of our resolved archaea-MAGs (Fig. 2; Additional file 3: Fig. S1). We showed that our methanogen populations had close phylogenetic relationships with archaea from geographically distinct mammalian hosts, suggesting high similarities in gene functions in archaea among diverse host species. Given similarities amongst such diverse host species with diverse digestive systems, we hypothesize these close genetic relatives of our resolved archaea-MAGs might be more ubiquitous in a wider range of hosts that are currently discussed. We noticed Ar-4 clustered, as expected, with 6 *Methanomethylophilus alvus* strains: 5 from human gut samples and 1 from swine (MAG221) (Fig. 2A) [31–36]. Ar-7 clustered with 4 *MX-02 sp006954405*. United Kingdom strain 10 [37] and Chinese strain MAG014 [34] have been identified as swine-originating, whereas B5_69.fa and B45_maxbin.030.fa were from humans [38]. Interestingly, clustering on the same branch (*B5_69.fa* and *B45_maxbin.030.fa*) are archaea isolated from South African adult humans [38]. Ar-1 was in the same branch with archaea from Tibetan pig MAG098 [34]; Ar-2 with Chinese roe deer RGIG3983 [39] strain; and Ar-3 with Tibetan pig MAG196 [34]. Likewise, we observed Ar-8 was on the

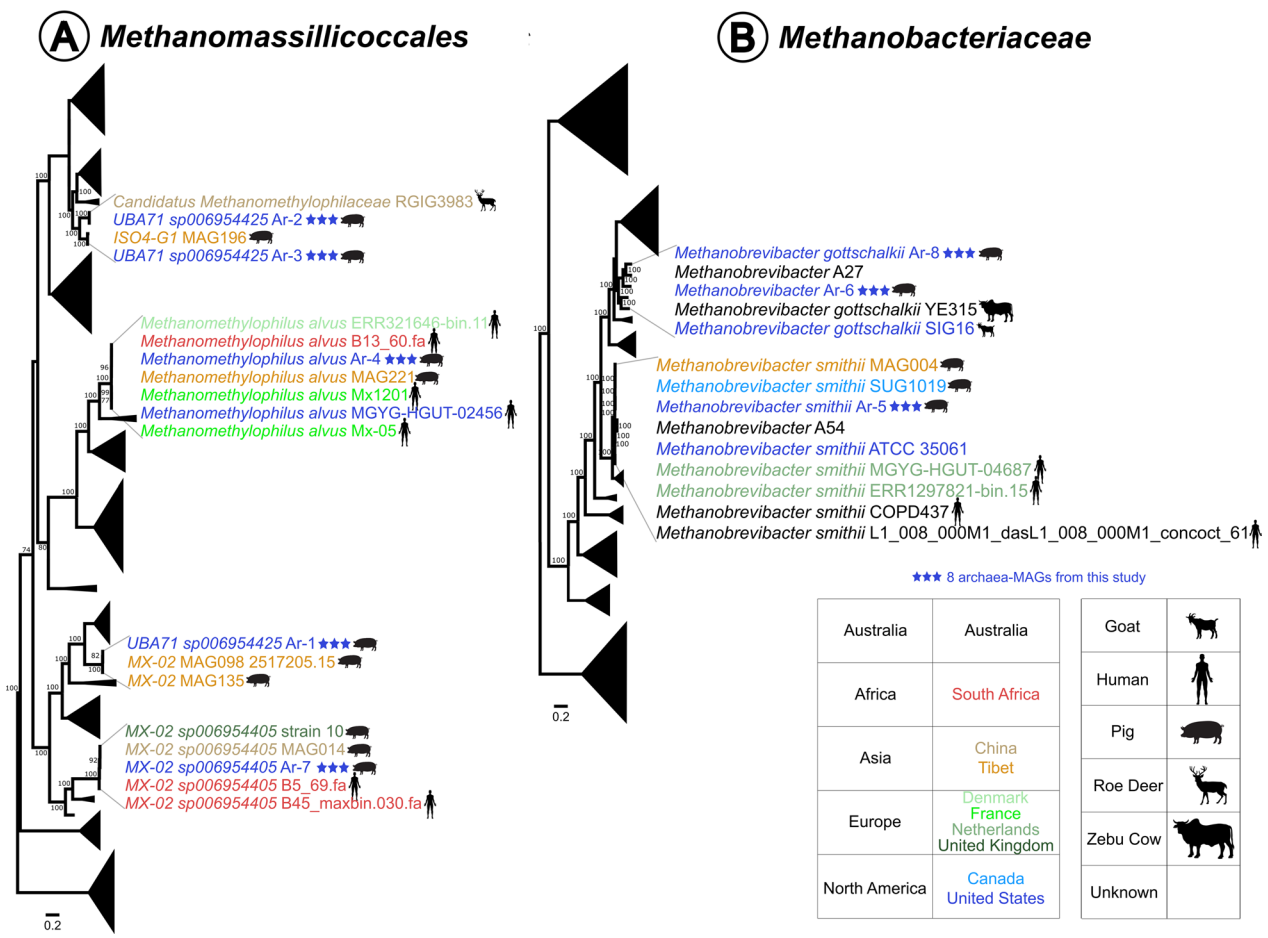

Fig. 2 Phylogenetic trees of **A** *Methanomassiliicoccales* [31–40] and **B** *Methanobacteriales* [34, 40–43, 45–50] with bootstrap values ≥ 70 indicated at nodes. Branches were collapsed for non-immediate phylogenetic relatives of our archaea-MAGs while branches containing these 8 MAGs were magnified for clarity. Original trees are in Additional file 3: Fig. S1

same phylogenetic branch with an Australian *Methanobrevibacter gottschalkii* isolate: A27 [40] (Fig. 2B). Interestingly, Ar-6 formed an outbranch alongside this branch with a further outbranch containing two *Methanobrevibacter gottschalkii* strains [41, 42]. This would suggest that our resolved archaea-MAG Ar-6 might be a *Methanobrevibacter gottschalkii*. Moreover, Ar-5 clustered amongst *Methanobrevibacter smithii* strains: Tibetan pig MAG004 [34], Canadian pig SUG1019 [43], and US Florida human ATCC 35061 [44]. We further performed pairwise average nucleotide identity (ANI) analysis on a subset of human-associated methanogen representatives [16], to determine genetic similarity between swine and human archaea. We found 4 nearly identical (99%) swine-human archaea MAG pairs: Ar-7 and GUT_GENOME284400; Ar-3 and GUT_GENOME233274; Ar-5 and GUT_GENOME194015; Ar-4 and GUT_GENOME201980. This finding although provided support for the differentiation of human and swine methanogen populations, it also highlights the archaeome of swine and human gut may be more similar than previously known.

While many of our methanogen MAGs clustered with swine originating archaea populations, we also demonstrated our methanogen MAGs alongside human and deer associated methanogens, suggesting similarities in microbial genes and associated functions in the methanogens amongst these host species. The roe deer similarity is especially intriguing considering that deer contain a ruminant digestive system, with four stomach compartments, compared to the single stomach system of monogastric swine and human [24, 51]. Moreover, even though our archaea-MAGs originated from the United States (in the state of Kansas) swine, our phylogenetic analyses indicated similarities to archaeal populations from Australia, South Africa, Tibet, China, United Kingdom and Canada, further supporting the global presence of archaea amongst diverse hosts. We surmise that our resolved methanogen archaea-MAGs and these close genetic relatives might be more widespread in more hosts than we expected [28].

We recovered from our study novel archaeal genomes that were previously unidentified in US swine. We were able to resolve and obtain the genomic information, to the best of our knowledge, of the first swine-associated *Methanobrevibacter UBA71 sp006954425* and *Methanobrevibacter gottschalkii* MAGs. The methanogenic archaea family *Methanobacteriales* has been identified in many previous swine studies, with the majority of these studies utilizing 16S sequencing and/or real-time PCR identification [34, 37, 52–61]. Still, there is a lack of understanding of the *Methanobacteriales* in terms of genomic studies, and the *Methanomassiliicoccales* order collectively in general. Up to this moment, only three swine *Methanomassiliicoccales* MAGs (*Methanomethylophilus alvus*, *MX-02 sp006954405*, and *Methanobrevibacter smithii*) have been identified [34, 37, 61]. Thus, adding our highly resolved novel archaea-MAGs to the repertoire of swine-associated microbial populations will aid in understanding swine archaea, including functions, host associations (such as age, health status, sex, etc.), and global distribution.

Prevalence of archaeal MAGs and variants at distinct host ages

Assessing the abundance of the methanogens in different growth stages of the swine host provided an opportunity to investigate the association between the host-associated methanogens and the different conditions faced by the swine as they grow. Our genome-centric metagenome analyses revealed two dominant orders of archaea—*Methanobacteriales* and *Methanomassiliicoccales*. We showed that resolved methanogen MAGs were differentially detected at different growth stages of the swine, but does the environment affect the functional niche specificity between these two orders of archaea?

The heatmap shown in Fig. 3A provides a graphical summary of the changes in detection for the archaea-MAGs. Detection was defined as the proportion of a given contig in the MAG that is covered at least 1X. Hierarchical clustering grouped the archaea-MAGs into three clusters based on detection: A (top cluster; Ar-1 through Ar-4), B (middle cluster; Ar-5 and Ar-6), and C (bottom cluster; Ar-7 and Ar-8). We observed that Cluster A contained only *Methanomassiliicoccales* MAGs, while Cluster B contained 2 *Methanobacteriales* MAGs, and Cluster C one of each order. Cluster A archaea-MAGs were primarily identified in the final stage of growth adult hosts. Conversely, Cluster B methanogens were primarily identified in preweaning hosts. Finally, Cluster C archaea were identified throughout the host lifetime. Further support of distinct archaea-MAGs detection was supported through archaeal-MAG relative abundances (Additional file 4: Fig. S2).

We noticed the majority of archaea-MAGs detection values increased closely after a stage transition (preweaning to nursery and nursery to growth adult), suggesting that stage transition changes, including diet, housing, and stress, can lead to changes in microbiome composition [62]. Although, exactly how these changes impact archaea is relatively understudied, as most research evaluates bacteria, and therefore archaea-stage dynamics are a topic for future research [63, 64].

We investigated methanogen variants, and found the majority of variation occurred in periods when other archaea were dominating (preweaning and growth adult; Additional file 5: Table S5). We

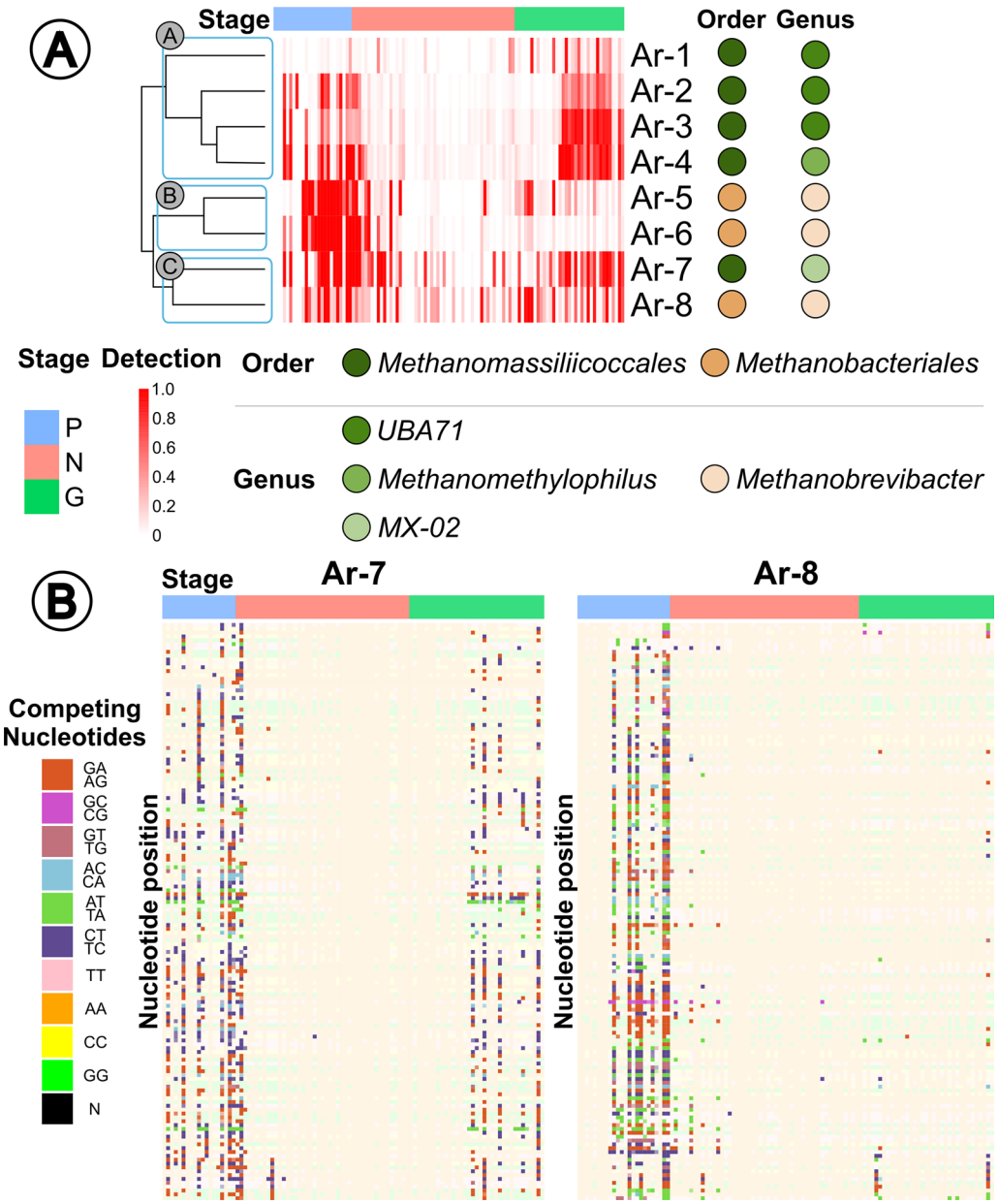

Fig. 3 **A** Detection (portion of MAG with at least 1X read coverage) heatmap of archaea-MAGs (rows) across all individual sample metagenomes (columns) with MAG taxonomy and stage annotation (Preweaning [P]; nursery [N]; growth adult [G]). **B** Single-nucleotide variant (SNV) analysis of Ar-7 and Ar-8 where box colors indicate competing nucleotides and stage is indicated along the bottom

performed single-nucleotide variant (SNV) analysis on our two archaea-MAGs that showed continuous detection throughout the host lifetime (Cluster C MAGs: Ar-7 and Ar-8; Fig. 3B). We attributed the majority of variances to the unweaned host, and fewer variances were identified in the growth adult. Interestingly, the number of variant populations were highest during times where other archaea-MAGs were predominantly identified (Fig. 3B). We hypothesized that the variation found in the growth adult host could indicate a competitive microbial environment, while fewer variants as compared to the earlier growth stages could be due to a largely already developed gut microbiome. In a competitive gut microbiome system, it is beneficial to have genetic diversity which translates to increased functional diversity [65]. A similar competitive environment and SNV diversity was demonstrated in the human gut bacterial community [65]. Comparatively, as the gut developed and

microbes established with focused functions, the variation decreased when humans reached 2 years of age [65]. Human preweaning gut development is similar to the development of the swine preweaning gut, albeit swine is relatively faster [66]. The conditions which encouraged the increased variation in the growth adult in our study could have been a change of diet, host stress, or other host-associated and environmental conditions [67].

While we demonstrated differing archaea and SNV association with age, we were primarily interested in methanogen function. We hypothesized methanogenic function influenced our resolved methanogen MAGs' ability to establish in the microbiome at different host stages through energy acquisition via host diet. Phylogenetic similarity in archaea across geography and hosts prompted an investigation into whether our archaea-MAGs were identified in other hosts of similar developmental ages, and therefore similar archaeal functions.

Methanogens span host species, millennia, and geographic distance

We wanted to further demonstrate not only global and host distribution, but also temporal, or across time, identification of our methanogens beyond genetic similarity, as illustrated in our phylogenetic analyses. We mapped metagenomic sequencing reads from young and aged hosts to our archaea-MAGs from the following hosts: swine (n = 16) [68], humans (n = 429) [69, 70], mice (n = 60) [71], chicken (n = 71) [72], and cattle (n = 34) [73] (Fig. 4; Additional files 6: Tables S6 and 7: Table S7). Our archaea-MAGs were identified in older humans and varying aged swine metagenomes, but not in the chicken, mice or cattle metagenomes. We also demonstrated evidence of our archaea-MAGs in the ancient human gut and global distribution. Altogether we determined within a host species, archaeal age-association appeared to be similar, but some archaea span multiple host species, and for millennia [28]. We hypothesized differential archaeal function may be essential to the gut microbiome of many modern and ancient monogastric hosts.

We determined our swine-associated methanogens were not present in poultry, mice and ruminant host metagenomes (Additional file 7: Table S7). Prescence of methanogens was determined when detection (portion of MAG with at least 1X read coverage) was greater than 0.25. This threshold aligns with previous genome-resolved metagenomic research and eliminated false-positive signals in read recruitment results [74–76]. Given the drastic differences in the ruminant digestive system compared to the monogastric gut, we were not surprised that our swine archaea-MAGs were not found in cattle from the United States (US) State of Pennsylvania. Although not identified consistently in all cattle, *Methanobrevibacter smithii* [77–80] and *Methanobrevibacter gottschalkii* [81–84] have been associated with the cow digestive tract. Similarly, *UBA71* has been identified in adult chickens previously [85]. Given that similar taxonomic methanogens are present in cattle and chickens, we hypothesized the methanogens of these hosts were genetically distinct from the methanogens we identified in swine. Additionally, since the methanogens we identified were not consistently detected across our aging hosts, it was very probable that other metagenomes from these host populations could contain our methanogens. Future research is necessary to evaluate how distinct methanogen members function individually and collectively within the microbiome system to influence gut health in different host species.

Interestingly, we could only find a singular example of archaea attributed to the mouse gut: *Methanomassiliicoccaceae DTU008* [86]. Remaining attempts, encompassing more than 1,000 metagenomes, proved unsuccessful in identifying mice gut archaea [87–90]. In fact, an investigation of murine gut composition across 17 rodent species demonstrated, beyond the instance of mouse *DTU008*, only North American porcupine (*Erethizon dorsatum*), capybara (*Hydrochoerus hydrochaeris*), and guinea pig (*Cavia porcellus*) contained archaea [86]. Although murine hosts have a monogastric digestive system, there appears to be a lack of understanding if and when archaea are present in mouse gut [90].

Although from a different continent, Chinese swine demonstrated the closest age-associated detection to our US swine methanogens. Even though the Chinese preweaning swine were not weaned, the methanogen presence appeared to more closely resemble the US swine weaned, nursery gut. The exception to the nursery resemblance being Ar-5, which more closely resembled our US swine preweaning gut. Many factors, including breed, weaning age (China at 42 days; US at 18–20 days), and housing, are known to influence microbiome development, and therefore could have resulted in the different archaeal age-establishment patterns [62, 91, 92]. In terms of our earlier detection clusters, Cluster A appeared more prevalent in the growth adult host, and Cluster C was similarly prevalent throughout both the preweaning and growth adult stages. Although the detections of Ar-5 and Ar-6 (Cluster B) were not shared between the Chinese and US swine, as Ar-6 demonstrated relatively low detection in the preweaning stage. Given that the Chinese swine dataset was from a single day in preweaning and growth adult, future research should investigate longitudinal distribution of methanogens from monogastric swine according to various characteristics, such as country of origin, breed, diet, housing environment, etc. This would further develop our understanding of

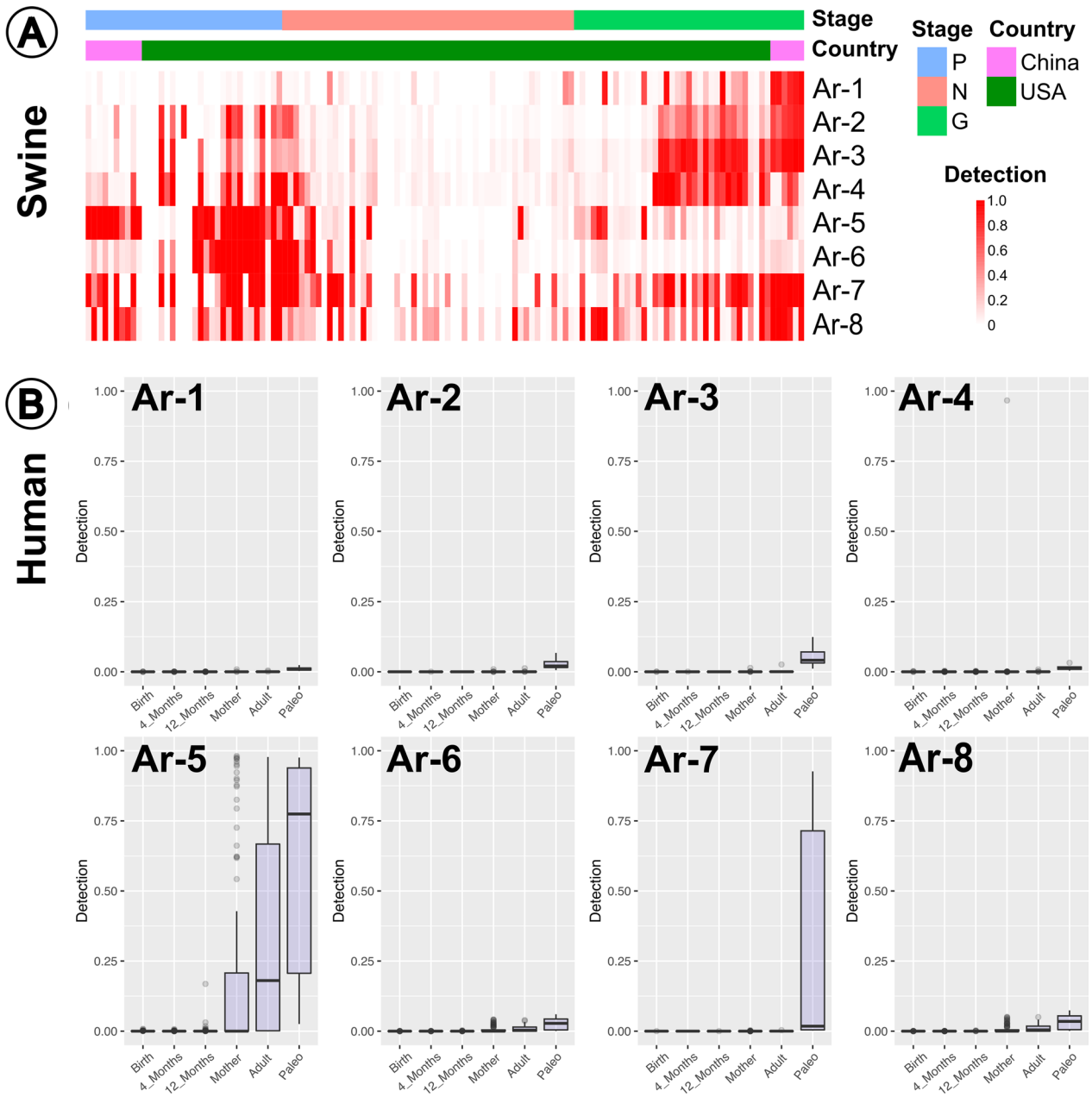

Fig. 4 **A** Detection (portion of MAG with at least 1 read coverage) heatmap of previously published swine metagenomes [68] mapped to this publication's archaeal MAGs (Preweaning [P]; nursery [N]; growth adult [G]). **B** Detection box plots of previously published human metagenomes [69, 70] mapped to our archaeal MAGs ("Adult" from Mexican humans; "Paleo" from present day US and Mexico; all remaining groups from Sweden)

global methanogen distribution according to associated variables.

Overall, we demonstrated genetic support for the same, or very closely related, methanogens circulating in both US and Chinese swine with similar age-associated detection. This further demonstrates the ubiquity of archaea to the monogastric swine host which we hypothesized are distributed with host age according to archaeal function.

Our resolved archaea-MAGs not only appeared in Chinese swine, but we also provided evidence of these archaea-MAGs in adult humans from modern age (Mexico and Sweden) and ancient time (modern day US and Mexico). In contrast to the swine gut, we identified merely two of our eight methanogens in the human gut: *M. smithii* and *MX-02 sp006954405*. With the exception of one Swedish 12-month sample demonstrating Ar-5

presence, the infant data illustrated comparatively minimal to no archaeal presence of our methanogens. Given that many publications demonstrate identification of multiple *Methanobacteriales* and *Methanomassiliicoccales* in the human gut [4, 6, 93, 94], it is possible that there were genetically distinct methanogens present in these human samples beyond our *M. smithii* and *MX-02 sp006954405*. The modern adult human samples, both the Mexican and Swedish datasets, only demonstrated *M. smithii* presence. Multiple publications have identified increasing *M. smithii* in the human gut with age [94, 95]. Interestingly, we identified *MX-02 sp006954405* and *M. smithii* in the palaeofaeces from the US and Mexico, suspected to be between 1000 and 2000 years old [69]. While many paleobiology studies have investigated ancient methanogens of water sediments [96–104], we identified merely two human-related paleobiology methanogen studies pertaining to: the archaic human gut [69] and neanderthal dental plaques [105]. *M. smithii* has been previously identified in ancient humans [69], but the identification of *MX-02 sp006954405* appeared to be the first evidence of human-associated ancient *Methanomassiliicoccales*. The methanogen *MX-02* has been identified in the human gut previously [16], but we illustrated novel evidence for *MX-02 sp006954405* in the ancient human gut, suggesting that *MX-02 sp006954405*, or close relatives, were likely present in the modernized human gut, but we did not identify genetic resemblance in the 122 modern human metagenomes we evaluated. Future research is necessary to provide further insights into the gut-associated archaea to elucidate genetic phylogeny, evolution of archaeal functions, and association with ancient humans.

Given our findings indicating our US-swine associated archaea-MAGs were present in Chinese swine, US humans, and Mexican humans, we wanted to further understand the role of these methanogens in the monogastric gut.

Critical methane metabolism functional potential were conserved across methanogens

Our primary goal was to profile the genomic potential that contributed to the methanogenesis of the swine gut. In our study, we constructed and demonstrated the first genetic support for a complete swine-associated acetoclastic methanogenic pathway, which is crucial for understanding the role of archaea within the microbiome system and to host health. We analyzed methanogenesis pathways of *Methanobacteriales*

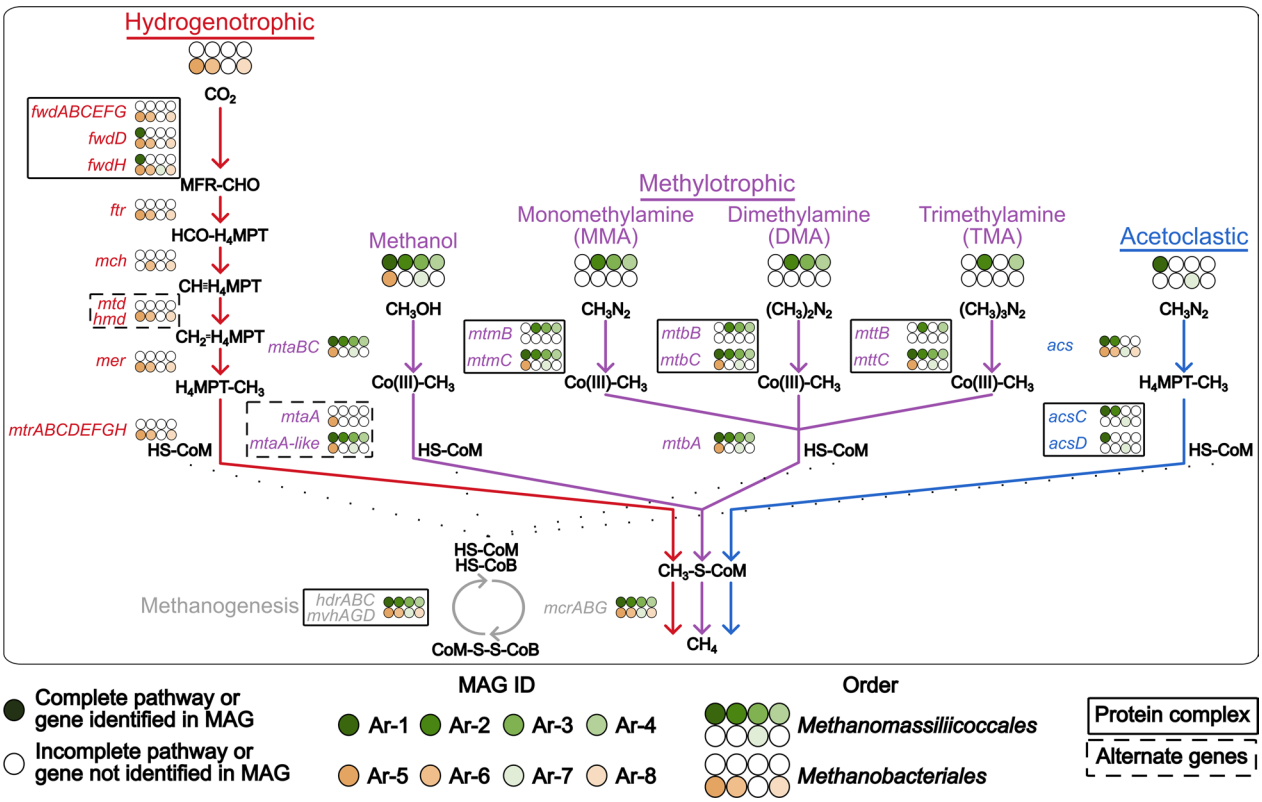

Fig. 5 Methane metabolic pathway genes detected in our archaeal MAGs distinguished by pathway [30, 118–120]

and *Methanomassiliicoccales* (Fig. 5, Additional file 2: Table S4). We identified 44 genes in methane metabolism [106].

The shared genes represented crucial functions in the final methanogenesis steps of energy and methane production. Nine genes were shared across the 8 archaea-MAGs: 3 heterodisulfide reductase (*hdrA*, *hdrB*, and *hdrC*), 3 methylviologen-dependent Ni,Fe hydrogenase (*mvhA*, *mvhG*, and *mvhD*), and 3 methyl-coenzyme M reductase (*mcrA*, *mcrB*, and *mcrG*). HdrABC, MvhAGD, and McrABG are critical to the final steps of methanogenesis. HdrABC and MvhAGD form an electron-bifurcating complex to regenerate coenzyme M (HS-CoM) and coenzyme B (HS-CoB) from heterodisulfide CoM-S-S-CoB [107]. An intermediate step, discussed in the following section even though the step is not shared by all archaea, generates methylated coenzyme M (CH_3-S-CoM) [25]. McrABG then catalyzes the final methanogenesis step where the methyl group of CoM-CH_3 is reduced to methane, with HS-CoB utilized as an electron donor [25]. This formation of methane generates CoM-S-S-CoB for reduction again by HdrABC/MvhAGD [108]. The final step in producing methane is crucial for methanogens, and our archaea-MAGs supported the roles of HdrABC, MvhAGD, and McrABC in these final methanogenesis reactions.

Differential methanobacteriales and methanomassiliicoccales methane metabolic pathways may relate to age-associated detection

While we supported the clear ubiquity of *hdr*, *mvh* and *mcr* to methanogens, we were primarily interested in how our archaea differed in methanogenic genes since they exhibited differential colonization through the swine growth stages. We noticed our taxonomically distinct archaea-MAGs harbored different genetic components for divergent methane metabolic pathways (Fig. 5). We identified the first genetic support of an acetoclastic *Methanomassiliicoccales*, and first acetoclastic methanogen in a monogastric host. Moreover, *Methanomassiliicoccales* also contained genes for the methylotrophic methanogenic pathway, indicating the potential to utilize various substrates from acetate to methylated compounds. Alternatively, *Methanobacteriales* contained genes for the hydrogenotrophic pathway with CO_2 as the substrate input. We surmised that these alternate pathways played a role in energy acquisition according to differential nutrients available during the host lifetime, and therefore growth stage associated diet.

The hydrogenotrophic methanogenic pathway was the key methanogenic pathway identified in all of our *Methanobacteriales* MAGs. During hydrogenotrophic methanogenesis, CO_2 is reduced to methane (CH_4) with four molecules of H_2 [25, 109]. Our *Methanobacteriales* archaea-MAGs contained all genes crucial to the hydrogenotrophic methanogenic pathway: formylmethanofuran dehydrogenase (*fwd*; A-H), formylmethanofuran-tetrahydromethanopterin N-formyltransferase (*ftr*), methenyltetrahydromethanopterin cyclohydrolase (*mch*), coenzyme F_{420}-dependent methylenetetrahydromethanopterin dehydrogenase (*mtd*), methenyltetrahydromethanopterin hydrogenase (*hmd*), methylenetetrahydromethanopterin reductase (*mer*), and methyltetrahydromethanopterin-coenzyme M methyltransferase (*mtr*; A-H) [30, 110].

We identified both *mtd* and *hmd*, indicating the methanogens can potentially utilize H_2 with or without F_{420} to reduce methenyl-H_4MPT, as Mtd requires F_{420} [111]. As mentioned previously, we believe the CH_3-CoM in our *Methanobacteriales* archaea-MAGs was generated via MtrABCDEFGH. This *mtr* complex has been demonstrated to transfer the methyl group from tetrahydromethanopterin (H_4MPT) to CoM, therefore coupling the hydrogenotrophic pathway to the final methane production steps [12, 112, 113]. *Methanobacteriales* have been associated with the hydrogenotrophic pathway previously [25].

Our *Methanobacteriales* archaea-MAGs contained all of the aforementioned genes, with one exception: Ar-5 lacked *mch*. We attribute this to the incompleteness of the metagenome-assembled genome, as Ar-5 exhibited the lowest completion of our methanogen MAGs at ~ 72% (Table 1, Additional file 1: Table S3). Interestingly, only two hydrogenotrophic pathway genes (*fwdD* and *fwdH*) were identified in two *Methanomassiliicoccales* archaea-MAGs. The lack of a hydrogenotrophic pathway clearly indicated the *Methanomassiliicoccales* utilized a distinct methane pathway.

All *Methanomassiliicoccales* archaea-MAGs, and our *M. smithii* archaea-MAGs, indicated varying ability to metabolize methanol, mono-, di- and trimethylamine through the methylotrophic methanogenesis pathway. Genes we identified in our archaea-MAGs included: methanol:coenzyme M methyltransferase (*mtaB* and *mtaC*), monomethylamine (MMA) methyltransferase (*mtmB* and *mtmC*), dimethylamine (DMA) methyltransferase (*mtbA*, *mtbB*, and *mtbC*), and trimethylamine (TMA) methyltransferase (*mttB* and *mttC*) [30]. *Methanomassiliicoccales* is known to perform methylotrophic methanogenesis with all of the previously discussed substrates [114]. Conversely, *M. smithii* was thought to be a hydrogenotrophic population [115]. Given we only identified methylotrophic genes in one *Methanobacteriales* population, future research is necessary to support this genetic potential.

Although all *Methanomassiliicoccales* methanogens and the *M. smithii* population contained the *mtaBC* genes for methanol metabolism, we did not identify *mtaA* in the *Methanomassiliicoccales* genetic content. The MtaABC complex transfers the methyl group from methanol to coenzyme M, generating CH_3-S-CoM for McrABG reduction [116]. We identified a candidate *mtaA* homolog through a literature review: uroporphyrinogen III decarboxylase (*hemE*) [117] (designated *mta-like* in Fig. 5 and Additional file 2: Table S4). This is the first publication identifying the homolog in methanogens. As such, future research is critical to analyze how HemE might interact with MtaBC, and how the enzyme performs in the methylotrophic pathway.

Only three (Ar-2, Ar-3, and Ar-4) out of the five *Methanomassiliicoccales* archaea-MAGs contained a complete genetic pathway associated with monomethylamine (*mtmBC*) and dimethylamine (*mtbBC*) utilization [30, 118]. Moreover, only two *Methanomassiliicoccales* populations (Ar-2 and Ar-4) contained *mttBC*, associated with trimethylamine (TMA) utilization [30, 118]. TMA has been associated with increased cardiovascular disease, so TMA metabolism is beneficial for the host [4, 5]. Further research is necessary to evaluate if other methylated compounds may play roles in cardiovascular disease, and therefore the host aided by archaeal metabolism. Although the majority of our archaea-MAGs appeared to be able to utilize methanol in the methylotrophic methanogenesis pathway, fewer were able to use mono-, di- and trimethylamine. As noted previously, this might be due to the incompleteness of the archaea-MAGs, especially since our *Methanomassiliicoccales* archaea-MAGs completeness ranged from ~ 80 to 99% (Table 1, Additional file 1: Table S3). Still, there is a possibility that these *Methanomassiliicoccales* archaea-MAGs might have different abilities in utilizing methylated sources due to contrasting biological necessity and evolutionary selection [121].

To the best of our knowledge, we identified the first complete acetoclastic methanogenic pathway in *Methanomassiliicoccales* [122, 123]. Three *Methanomassiliicoccales* (Ar-1, Ar-2, and Ar-7) archaea-MAGs contained genetic support, with two complete pathways (Ar-1 and Ar-7), for the acetoclastic, or also called aceticlastic, pathway. Acetate is reduced to acetyl-CoA and then H_4MPT via acetyl-CoA synthetase (*acs*) and carbon monoxide dehydrogenase (*acsC* and *acsD*) [30, 118, 124]. Two of our *Methanomassiliicoccales* archaea-MAGs (Ar-3 and Ar-4) did not have acetoclastic genes identified, while *acsD* was not found in Ar-2.

Acetoclastic methanogenesis is typically performed by aquatic methanogens [125–127]. The only prior identification of acetoclastic archaea in gastrointestinal tracts was in *Methanosarcinales* of a ruminant host (cow) [4, 128]. Therefore, we identified the first evidence for acetoclastic methanogenesis in monogastrics. Moreover, only *Methanosarcinales* and *Methanococcales* were known to perform acetoclastic methanogenesis [122, 128, 129]. The ability of our *Methanomassiliicoccales* to perform both methylotrophic and acetoclastic methanogenesis parallels *Methanosarcinales*, since many *Methanosarcinales* also are able to perform both of these pathways [123]. Conversely, acetoclastic-able *Methanococcales* are also able to perform hydrogenotrophic methanogenesis [128]. Acetoclastic methanogenesis requires an ATP input to convert acetate to acetyl-CoA, which impairs the energy efficiency of this methanogenic pathway [130]. The diminished energy return of acetoclastic methanogenesis likely plays a role in the dual acetoclastic-methylotrophic metabolic potential of our *Methanococcales* archaea-MAGs. The ability to utilize different substrates via varying methanogenic pathways is beneficial. The methanogen can potentially still metabolize energy as their substrate source changes. Changing substrates is common in the gastrointestinal system, as the host changes diets and the associated microbiome changes and produces different metabolites [63].

Although the *Methanomassiliicoccales* archaea-MAGs contained genes for both methylotrophic and acetoclastic methanogenesis, this dynamic substrate capability did not appear to allow *Methanomassiliicoccales* archaea-MAGs to prevail more than their counterparts: *Methanobacteriales*. In fact, the *Methanobacteriales* populations in general were detected at more times during the host life than *Methanomassiliicoccales* (Fig. 3A). This may indicate CO_2 is more available in the monogastric system during the host lifetime. The exception to this being the during the growth stage where *Methanomassiliicoccales* appear abundantly, therefore methylated compounds or acetate could have transitioned to being the dominantly available substrate, suggesting that the stage-associated characteristics, such as dietary composition had a high influence on the methanogens dynamics. Although diet influences substrate availability, we cannot rule out other factors, including host age and other gastrointestinal organisms (including bacteria and protist), which alter the gut microbiome system [4, 63, 128, 131].

Collectively, with the novel acetoclastic *Methanomassiliicoccales* and methylotrophic *Methanobacteriales M. smithii* archaea-MAGs, there is a knowledge gap surrounding the functional potential of methanogens. Taken together with the phylogenetic analysis, we are lacking a holistic understanding from global and host distribution of methanogens to their methanogenic actions. Other publications have also discussed the lack of overall methanogen knowledge, especially knowledge surrounding

archaeal functions [132–134]. Future research should aim to cultivate archaea populations to further elucidate archaea characteristics and especially methanogenic potential. Although metagenome-assembled genome (MAG) analysis provides valuable genetic information, there is the potential for inaccurate gene association [135]. We performed manual binning curation to minimize these, but isolation cultivation would allow individual sequencing to further associate specific genes with archaea. Archaea are a member of the gut microbiome alongside bacteria, fungi and viruses, and without understanding their distribution and functions, we will not understand how archaea influence the gut microbiome system and host health.

Conclusions

We performed a longitudinal study of the monogastric microbiome where we produced 1,130 MAGs, with 8 methanogen archaea-MAGs. The novel archaea-MAGs clustered with geographically diverse methanogens from various animal and human hosts, indicating global distribution of closely related archaea. We also determined that our archaea-MAGs were detected in swine and humans from distinct continents and time. Given the stark distinctions in detection and distribution, we wanted to evaluate if energy acquisition associated with methanogenesis could be related to these factors, especially age-distribution. Our *Methanobacteriales* archaea-MAGs contained genes for hydrogenotrophic methanogenesis, indicating the ability to metabolize CO_2. Alternatively, *Methanomassiliicoccales* archaea-MAGs appeared to have the capability to utilize a range of substrates from methylated compounds, including methanol and methylamine, and acetate, through the methylotrophic and acetoclastic pathways, respectively. We identified the first acetoclastic *Methanomassiliicoccales*, and also the first acetoclastic methanogens of monogastrics. Moreover, we identified a *Methanobacteriales* population with methylotrophic genes. Previously, *Methanobacteriales* was thought to only perform hydrogenotrophic methanogenesis. We hypothesized the distinct diets, given according to age, provided different substrates which influenced archaeal establishment and therefore detection patterns. Still, we know there are multiple other growth stage-associated and microbiome dynamics which likely play a role in archaeal growth.

In order to continue developing our understanding of archaea, we must continue to evaluate their global prevalence across diverse hosts and ecosystems. Moreover, we should evaluate the significance of acetoclastic methanogens to monogastrics, including how these methanogens influence other microorganisms and host health. Future studies should also investigate how growth stage-associated factors influence methanogenic potential and therefore archaeal abundance. In pursuing this archaea research, we can better determine how methanogens provide beneficial or detrimental consequences to host health, and how we might utilize or deter methanogens in animals and humans alike.

Materials and methods

Study design, sample collection and DNA extraction

Our study design and sample collection occurred as previously described [136]. We collected fecal samples from 7 swine over 22 timepoints, ranging in swine age from 1 to 156 days across three developmental stages: preweaning (P), nursery (N), and growth adult (G) (Fig. 1, Additional file 8: Table S1). Swine were born and raised at the Kansas State University Swine Teaching and Research Center. Swine originated from the same farrowing group, and were weaned between 18 and 20 days of age, depending on day of birth.

We stored fecal samples at − 80 °C until DNA extraction. We extracted total genomic DNA from fecal samples utilizing the E.Z.N.A.® Stool DNA Kit (Omega Bio-tek Inc.; Norcross, GA), following the manufacturer protocols. We then quantified the extracted genomic DNA with a Nanodrop and Qubit™ (dsDNA BR Assay Kit [Thermo Fisher; Waltham, MA]) for DNA quality and concentration. We stored extracted DNA at − 80 °C until library preparation and sequencing.

Metagenomic sequencing and 'omics workflow

DNA libraries were generated for a total of 112 samples with Nextera DNA Flex (Illumina, Inc.; San Diego, CA). Resulting libraries were then visualized on a Tapestation 4200 (Agilent; Santa Clara, CA) and size-selected using the BluePippin (Sage Science; Beverly, MA). The final library pool of 112 samples was quantified on the Kapa Biosystems (Roche Sequencing; Pleasanton, CA) qPCR protocol, and sequenced on the Illumina NovaSeq S1 chip (Illumina, Inc.; San Diego, CA) with a 2 × 150 bp paired-end sequencing strategy.

We utilized the 'anvi-run-workflow' program to run a combined bioinformatics workflow in anvi'o v.7.1 (https://anvio.org/install/) [137, 138], with a co-assembling strategy. The workflow used Snakemake to implement numerous tasks including: short-read quality filtering, assembly, gene calling, functional annotation, hidden Markov model search, metagenomic read-recruitment and binning [139]. Briefly, we processed sequencing reads using anvi'o's 'iu-filer-quality-minoche' program, which removed low-quality reads following criteria outlined in Minoche et al. [140]. The resulting quality-control reads were termed "metagenome" per sample. We organized the samples into

3 metagenomic groups based on the developmental stages (P, N, G), and used anvi'o's MEGAHIT v1.2.9 to co-assemble quality-filtered short reads into longer contiguous sequences (contigs) [137, 141]. The following methods were then utilized in anvi'o to further process the contigs: (1) 'anvi-gen-contigs-database' to compute k-mer frequencies and identify open reading frames (ORFs) using Prodigal v2.6.3 [137, 142]; (2) 'anvi-run-hmms' to annotate bacterial and archaeal single-copy, core genes with default single-copy genes and taxonomy of genomes [143] as defined by the The Genome Taxonomy Database (GTDB) [144] database (Archaea_76, Bacteria_71, Protista_83, and Ribosomal RNAs) [145] using HMMER v.3.2.1 [137, 146]; (3) 'anvi-run-ncbi-cogs' to annotate ORFs with NCBI's Clusters of Orthologous Groups (COGs; https://www.ncbi.nlm.nih.gov/research/cog) [147]; and (4) 'anvi-run-kegg-kofams' to annotate ORFs from KOfam HMM databases of KEGG orthologs (https://www.genome.jp/kegg/) [148].

We mapped metagenomic short reads to contigs in anvi'o with Bowtie2 v2.3.5 [149], and we then converted mappings to BAM files with samtools v1.9 [137, 150, 151]. We used the anvi'o 'anvi-profile' program to profile BAM files with a minimum contig length of 1000 bp. Next, we combined profiles with 'anvi-merge' into a single anvi'o profile for downstream analyses. We grouped contigs into bins with 'anvi-cluster-contigs' and CONCOCT v1.1.0 [152]. We manually processed bins with 'anvi-refine' using bin tetranucleotide frequency and coverage across samples [137, 153, 154]. Following manual processing, we labeled bins that had > 70% completion and < 10% redundancy (both based on single-copy core gene annotation) as metagenome-assembled genomes (MAGs). Finally, we used 'anvi-compute-genome-similarity' to calculate average nucleotide identity (ANI), using PyANI v0.2.9 [137, 155], for each MAG to identify non-redundant MAGs. We analyzed MAG occurrence in a sample with the "detection" metric. We considered a MAG as detected in a metagenome if the detection was > 0.25, which is an appropriate cutoff to eliminate false-positive signals in read recruitment results [74–76]. Detection described the portion of MAG with at least one read mapped to a nucleotide, or minimum 1X coverage [156]. We used 'anvi-gen-variability-profile' with '–quince-mode' to export single-nucleotide variant (SNV) information on all MAGs after read recruitment, to identify subpopulations of the MAGs in the metagenomes [137]. We used DESMAN v2.1.1 in anvi'o to analyze the SNVs and determine the number and distribution of subpopulations in the MAGs [157]. We accounted for non-specific mapping by removing any subpopulations that made up less than 1% of the entire population that were explained by a single MAG.

Data analyses

We used the "detection" criteria (> 0.25) for downstream statistical analyses. We downloaded metagenomes from swine [68], humans [69, 70], mice [71], chicken [72], and cattle [73], and performed mapping to the non-redundant archaea-MAGs according to specifications above (Additional file 9: Table S2). We used RStudio v1.3.1093 [158] (https://www.rstudio.com/products/rstudio/) to visualize MAGs detection patterns using: pheatmap (pretty heatmaps) v1.0.12 [159], ggplot2 v3.3.5 (https://ggplot2.tidyverse.org/) [160], forcats v0.5.1 (https://forcats.tidyverse.org/) [161], dplyr v1.0.8 (https://dplyr.tidyverse.org/) [162], and ggpubr v0.4.0 (https://CRAN.R-project.org/package=ggpubr) [163].

We utilized the RASTtk Genome Annotation Service on PATRIC v3.6.12 (https://patricbrc.org/) and anvi'o COG annotations for metabolic function analyses [164, 165]. We used the comparative pathway tool in PATRIC to predict the metabolic pathways of our resolved non-redundant MAGs. We used 'anvi-compute-genome-similarity' to calculate average nucleotide identity (ANI) with a subset of samples (n = 21) from previously published human-associated archaea [16]. We obtained similar genomes that were deposited in public databases and performed phylogenetic analyses of our non-redundant MAGs in PATRIC [165]. Parameters were set as follows: 100 genes, 10 max allowed deletions, and 10 max allowed duplications. We constructed phylogenetic trees for our MAGs with 192 closely related genomes, using the amino acid and nucleotide sequences from the global protein families database. RAxML program was used to construct the trees based on pairwise differences between the aligned protein families of the selected sequences.

Our final figures were edited in Inkscape v1.2.1 [166].

Supplementary Information

The online version contains supplementary material available at https://doi.org/10.1186/s42523-023-00256-6.

Additional file 1: Table S3. Anvi'o results from initial bins and resulting redundant and nonredundant MAGs, including taxonomic classification detailing archaeal MAGs and PATRIC genome IDs [137].

Additional file 2: Table S4. PATRIC RAStk and COGG gene annotations for methanogen MAGs.

Additional file 3: Fig. S1. Complete, non-collapsed, *Methanobacteriales* and *Methanomassiliicoccales* phylogenetic trees with statistics.

Additional file 4: Fig. S2: Relative abundance of archaea-MAGs (rows) across all individual sample metagenomes (columns) (Preweaning [P]; nursery [N]; growth adult [G]).

Additional file 5: Table S5. Single nucleotide variant (SNV) results.

Additional file 6: Table S6. Metadata from metagenomes utilized in mapping to our archaeal MAGs (swine [62], human infant [64], human adult and palaeofaeces [63], mice [65], chicken [66], and cattle [67]).

Additional file 7: Table S7. Detection results from metagenome mapping to archaea-MAGs.

Additional file 8: Table S1. Demographics (diet, birth date, housing group, etc.) of swine hosts and dams, and sample metadata (swine age, host ID, stage and general health information, etc.).

Additional file 9: Table S2. Sequencing and assembly analysis including: metagenomic read counts initially obtained and assembly statistics according to co-assembly stage.

Acknowledgements
Our team is very grateful to the large number of individuals and organizations which assisted us in performing this research. We thank members of the Kansas State University swine team (Frank Martin, Mark Nelson, Duane Baughman, and Julia Holen) for aiding in the sample collection. Gratitude is also extended to the University of Kansas Medical Center Genome Sequencing Facility for their expertise and assistance in sequencing including: Clark Bloomer, Dr. Veronica Cloud, Rosanne Skinner, and Yafen Niu.

Author contributions
BF, RG and STML designed the study. Sample collection was performed by BF. BF, VD, KR, KW, and SP completed DNA extraction and Nanodrop and Qubit quality analysis. BF and QR performed anvi'o and PATRIC bioinformatic analyses. BF and STML attributed biological relevance, wrote the manuscript, prepared figures, and Additional files. BF and STML performed major manuscript and figure refinement while remaining authors contributed to lighter refinement. MC provided valuable insights which aided in study progression and manuscript preparation. All authors read, contributed to manuscript revision, and approved the submitted version.

Funding
We greatly appreciate assistance from the following sources: Kansas State University Interdepartmental Genetics Program (fellowship for Brandi Feehan), Global Food Systems Seed Grant Program, Kansas Intellectual and Developmental Disabilities Research Center (NIH U54 HD 090216), the Molecular Regulation of Cell Development and Differentiation—COBRE (P30 GM122731-03)—the NIH S10 High-End Instrumentation Grant (NIH S10OD021743) and the Frontiers CTSA Grant (UL1TR002366) at the University of Kansas Medical Center, Kansas City, KS 66160.

Availability of data and materials
We uploaded our metagenome raw sequencing data to the SRA under NCBI BioProject PRJNA798835. All other analyzed data, in the form of databases and fasta files, and bioinformatic scripts are accessible at figshare https://doi.org/10.6084/m9.figshare.20431713.

Declarations

Ethical approval and consent to participate
Pigs were managed according to the Kansas State University Institutional Animal Care and Use Committee (IACUC) approved protocol #4036, and methods are reported according to ARRIVE guidelines. The authors also confirmed that all methods were performed in accordance with relevant guidelines and regulations, and we affirmed that all methods were approved by Kansas State University.

Competing interests
The authors declare no competing interests.

Author details
[1]Division of Biology, College of Arts and Sciences, Kansas State University, Manhattan, KS 66506, USA. [2]Department of Animal Sciences and Industry, College of Agriculture, Kansas State University, Manhattan, KS 66506, USA. [3]Swine Health Information Center, Ames, IA 50010, USA.

Received: 16 January 2023 Accepted: 11 July 2023
Published online: 17 July 2023

References

1. Coyte KZ, Rakoff-Nahoum S. Understanding competition and cooperation within the mammalian gut microbiome. Curr Biol. 2019;29:R538–44.
2. Shanahan F, Ghosh TS, O'Toole PW. The healthy microbiome-what is the definition of a healthy gut microbiome? Gastroenterology. 2021;160:483–94.
3. Aldars-García L, Chaparro M, Gisbert JP. Systematic review: the gut microbiome and its potential clinical application in inflammatory bowel disease. Microorganisms. 2021;9:5.
4. Gaci N, Borrel G, Tottey W, O'Toole PW, Brugère J-F. Archaea and the human gut: new beginning of an old story. World J Gastroenterol. 2014;20:16062–78.
5. Nkamga VD, Henrissat B, Drancourt M. Archaea: essential inhabitants of the human digestive microbiota. Human Microbiome Journal. 2017;3:1–8.
6. Kim JY, et al. The human gut archaeome: identification of diverse haloarchaea in Korean subjects. Microbiome. 2020;8:114.
7. Wampach L, et al. Colonization and succession within the human gut microbiome by archaea, bacteria, and microeukaryotes during the first year of life. Front Microbiol. 2017;8:738.
8. Pimentel M, et al. Methane production during lactulose breath test is associated with gastrointestinal disease presentation. Dig Dis Sci. 2003;48:86–92.
9. Ghoshal UC, Srivastava D, Verma A, Misra A. Slow transit constipation associated with excess methane production and its improvement following rifaximin therapy: a case report. J Neurogastroenterol Motil. 2011;17:185–8.
10. Samuel BS, Gordon JI. A humanized gnotobiotic mouse model of host-archaeal-bacterial mutualism. Proc Natl Acad Sci U S A. 2006;103:10011–6.
11. Brugère J-F, et al. Archaebiotics: proposed therapeutic use of archaea to prevent trimethylaminuria and cardiovascular disease. Gut Microbes. 2014;5:5–10.
12. Wang Y, et al. A methylotrophic origin of methanogenesis and early divergence of anaerobic multicarbon alkane metabolism. Sci Adv. 2021;7:1453.
13. Guy L, Ettema TJG. The archaeal "TACK" superphylum and the origin of eukaryotes. Trends Microbiol. 2011;19:580–7.
14. Vigneron A, Cruaud P, Lovejoy C, Vincent WF. Genomic evidence of functional diversity in DPANN archaea, from oxic species to anoxic vampiristic consortia. ISME Commun. 2022;2:1–10.
15. Oren A. Euryarchaeota. eLS 1–17 Preprint at https://doi.org/10.1002/9780470015902.a0004243.pub3 (2019).
16. Chibani CM, et al. A catalogue of 1,167 genomes from the human gut archaeome. Nat Microbiol. 2022;7:48–61.
17. Houshyar Y, Massimino L, Lamparelli LA, Danese S, Ungaro F. Going beyond bacteria: uncovering the role of archaeome and mycobiome in inflammatory bowel disease. Front Physiol. 2021;12:783295.
18. Yang K, et al. IDDF2021-ABS-0130 dysbiosis of gut archaea in obesity recovered after bariatric surgery. Gut. 2021;70:A46–A46.
19. Buan NR. Methanogens: pushing the boundaries of biology. Emerg Top Life Sci. 2018;2:629–46.
20. Gemperli AC, Dimroth P, Steuber J. Sodium ion cycling mediates energy coupling between complex I and ATP synthase. Proc Natl Acad Sci U S A. 2003;100:839–44.
21. Grüber G, Manimekalai MSS, Mayer F, Müller V. ATP synthases from archaea: the beauty of a molecular motor. Biochim Biophys Acta. 2014;1837:940–52.
22. Roswall J, et al. Developmental trajectory of the healthy human gut microbiota during the first 5 years of life. Cell Host Microbe. 2021;29:765-776.e3.
23. Hanachi M, et al. Longitudinal and comparative analysis of gut microbiota of tunisian newborns according to delivery mode. Front Microbiol. 2022;13:780568.

24. Saengkerdsub S, Ricke SC. Ecology and characteristics of methanogenic archaea in animals and humans. Crit Rev Microbiol. 2014;40:97–116.
25. Berghuis BA, et al. Hydrogenotrophic methanogenesis in archaeal phylum Verstraetearchaeota reveals the shared ancestry of all methanogens. Proc Natl Acad Sci U S A. 2019;116:5037–44.
26. Poretsky R, Rodriguez-R LM, Luo C, Tsementzi D, Konstantinidis KT. Strengths and limitations of 16S rRNA gene amplicon sequencing in revealing temporal microbial community dynamics. PLoS ONE. 2014;9:e93827.
27. Beauchemin KA, Ungerfeld EM, Eckard RJ, Wang M. Review: Fifty years of research on rumen methanogenesis: lessons learned and future challenges for mitigation. Animal. 2020;14:s2–16.
28. Thomas CM, Desmond-Le Quéméner E, Gribaldo S, Borrel G. Factors shaping the abundance and diversity of the gut archaeome across the animal kingdom. Nat Commun. 2022;13:3358.
29. Steinberg LM, Regan JM. mcrA-targeted real-time quantitative PCR method to examine methanogen communities. Appl Environ Microbiol. 2009;75:4435–42.
30. Qian L, et al. MCycDB: a curated database for comprehensively profiling methane cycling processes of environmental microbiomes. Mol Ecol Resour. 2022;22:1803–23.
31. PATRIC B13_60.fa. https://patricbrc.org/view/Genome/2774294.14.
32. PATRIC ERR321646-bin.11. https://patricbrc.org/view/Genome/1291540.8.
33. Guillaume B, et al. Genome sequence of "candidatus methanomethylophilus alvus" Mx1201, a methanogenic archaeon from the human gut belonging to a seventh order of methanogens. J Bacteriol. 2012;194:6944–5.
34. Zhou S, et al. Characterization of metagenome-assembled genomes and carbohydrate-degrading genes in the gut microbiota of tibetan pig. Front Microbiol. 2020;11:595066.
35. PATRIC MGYG-HGUT-02456. https://patricbrc.org/view/Genome/1291540.6.
36. PATRIC Mx-05. https://patricbrc.org/view/Genome/1291540.4.
37. Deng F, et al. Weaning time affects the archaeal community structure and functional potential in pigs. Front Microbiol. 2022;13:845621.
38. Tamburini FB, et al. Short- and long-read metagenomics of urban and rural South African gut microbiomes reveal a transitional composition and undescribed taxa. Nat Commun. 2022;13:926.
39. Xie F, et al. An integrated gene catalog and over 10,000 metagenome-assembled genomes from the gastrointestinal microbiome of ruminants. Microbiome. 2021;9:137.
40. Rinke C, et al. Validation of picogram- and femtogram-input DNA libraries for microscale metagenomics. PeerJ. 2016;4:e2486.
41. PATRIC YE315. https://patricbrc.org/view/Genome/1609968.3.
42. Peng X, et al. Genomic and functional analyses of fungal and bacterial consortia that enable lignocellulose breakdown in goat gut microbiomes. Nat Microbiol. 2021;6:499–511.
43. Holman DB, Gzyl KE, Mou KT, Allen HK. Weaning age and its effect on the development of the swine gut microbiome and resistome. MSystems. 2021;6:e0068221.
44. Samuel BS, et al. Genomic and metabolic adaptations of *Methanobrevibacter smithii* to the human gut. Proc Natl Acad Sci U S A. 2007;104:10643–8.
45. PATRIC A54. https://patricbrc.org/view/Genome/1860156.3.
46. PATRIC MGYG-HGUT-04687. https://patricbrc.org/view/Genome/2173.814.
47. PATRIC ERR1297821-bin.15. https://patricbrc.org/view/Genome/2173.815.
48. Bowerman KL, et al. Disease-associated gut microbiome and metabolome changes in patients with chronic obstructive pulmonary disease. Nat Commun. 2020;11:5886.
49. Lou YC, et al. Infant gut strain persistence is associated with maternal origin, phylogeny, and functional potential including surface adhesion and iron acquisition. *bioRxiv;* 2021. https://doi.org/10.1101/2021.01.26.428340.
50. PATRIC ATCC 35061. https://patricbrc.org/view/Genome/420247.28.
51. Prins RA, Geelen MJH. Rumen characteristics of red deer, fallow deer, and roe deer. J Wildl Manage. 1971;35:673–80.
52. Yeast-Derived β-1,3-Glucan Substrate Significantly Increased the Diversity of Methanogens During In vitro Fermentation of Porcine Colonic Digesta. J Integr Agric **12**, 2229–2234 (2013).
53. Luo Y, et al. Dietary pea fiber increases diversity of colonic methanogens of pigs with a shift from Methanobrevibacter to Methanomassiliicoccus-like genus and change in numbers of three hydrogenotrophs. BMC Microbiol. 2017;17:17.
54. Mi J, Peng H, Wu Y, Wang Y, Liao X. Diversity and community of methanogens in the large intestine of finishing pigs. BMC Microbiol. 2019;19:83.
55. Mao S-Y, Yang C-F, Zhu W-Y. Phylogenetic analysis of methanogens in the pig feces. Curr Microbiol. 2011;62:1386–9.
56. Luo Y-H, et al. Lean breed Landrace pigs harbor fecal methanogens at higher diversity and density than obese breed Erhualian pigs. Archaea. 2012;2012:605289.
57. Su Y, Bian G, Zhu Z, Smidt H, Zhu W. Early methanogenic colonisation in the faeces of Meishan and Yorkshire piglets as determined by pyrosequencing analysis. Archaea. 2014;2014:547908.
58. Federici S, et al. Archaeal microbiota population in piglet feces shifts in response to weaning: Methanobrevibacter smithii is replaced with Methanobrevibacter boviskoreani. FEMS Microbiol Lett. 2015;362:64.
59. Cao Z, et al. Effect of dietary fiber on the methanogen community in the hindgut of Lantang gilts. Animal. 2016;10:1666–76.
60. Bin P, et al. Effects of different levels of methionine on sow health and plasma metabolomics during late gestation. Food Funct. 2018;9:4979–88.
61. Crossfield M, et al. Archaeal and bacterial metagenome-assembled genome sequences derived from pig feces. Microbiol Resour Announc. 2022;11:e0114221.
62. Aluthge ND, et al. BOARD INVITED REVIEW: the pig microbiota and the potential for harnessing the power of the microbiome to improve growth and health. J Anim Sci. 2019;97:3741–57.
63. Hoffmann C, et al. Archaea and fungi of the human gut microbiome: correlations with diet and bacterial residents. PLoS ONE. 2013;8:e66019.
64. Patil Y, Gooneratne R, Ju X-H. Interactions between host and gut microbiota in domestic pigs: a review. Gut Microbes. 2020;11:310–34.
65. Vatanen T, et al. Genomic variation and strain-specific functional adaptation in the human gut microbiome during early life. Nat Microbiol. 2019;4:470–9.
66. Chen L, et al. The maturing development of gut microbiota in commercial piglets during the weaning transition. Front Microbiol. 2017;8:1688.
67. Qin Y, et al. Combined effects of host genetics and diet on human gut microbiota and incident disease in a single population cohort. Nat Genet. 2022;54:134–42.
68. Chen C, et al. Expanded catalog of microbial genes and metagenome-assembled genomes from the pig gut microbiome. Nat Commun. 2021;12:1106.
69. Wibowo MC, et al. Reconstruction of ancient microbial genomes from the human gut. Nature. 2021;594:234–9.
70. Bäckhed F, et al. Dynamics and stabilization of the human gut microbiome during the first year of life. Cell Host Microbe. 2015;17:690–703.
71. Jovel J, et al. Metagenomics versus metatranscriptomics of the murine gut microbiome for assessing microbial metabolism during inflammation. Front Microbiol. 2022;13:829378.
72. Segura-Wang M, Grabner N, Koestelbauer A, Klose V, Ghanbari M. Genome-resolved metagenomics of the chicken gut microbiome. Front Microbiol. 2021;12:726923.
73. Haley BJ, Kim S-W, Salaheen S, Hovingh E, Van Kessel JAS. Differences in the microbial community and resistome structures of feces from preweaned calves and lactating dairy cows in commercial dairy herds. Foodborne Pathog Dis. 2020;17:494–503.
74. Watson AR, et al. Metabolic independence drives gut microbial colonization and resilience in health and disease. Genome Biol. 2023;24:78.
75. Delmont TO. Binning giant viruses and their close relatives with anvi'o. *Meren Lab* https://merenlab.org/2022/01/03/giant-viruses/.
76. Metapangenomics of Rothia and H. parainfluenzae. Daniel Utter (2023). https://dutter.github.io/projects/oral_metapan.
77. Wright A-DG, Auckland CH, Lynn DH. Molecular diversity of methanogens in feedlot cattle from Ontario and Prince Edward Island. Canada Appl Environ Microbiol. 2007;73:4206–10.

78. Zhou M, Hernandez-Sanabria E, Guan LL. Characterization of variation in rumen methanogenic communities under different dietary and host feed efficiency conditions, as determined by PCR-denaturing gradient gel electrophoresis analysis. Appl Environ Microbiol. 2010;76:3776–86.
79. Danielsson R, Schnürer A, Arthurson V, Bertilsson J. Methanogenic population and CH4 production in Swedish dairy cows fed different levels of forage. Appl Environ Microbiol. 2012;78:6172–9.
80. Skillman LC, Evans PN, Strömpl C, Joblin KN. 16S rDNA directed PCR primers and detection of methanogens in the bovine rumen. Lett Appl Microbiol. 2006;42:222–8.
81. Hernandez-Sanabria E, et al. Influence of sire breed on the interplay among rumen microbial populations inhabiting the rumen liquid of the progeny in beef cattle. PLoS ONE. 2013;8:e58461.
82. Malik PK, et al. Comparison of enteric methane yield and diversity of ruminal methanogens in cattle and buffaloes fed on the same diet. PLoS ONE. 2021;16:e0256048.
83. McCabe MS, et al. Illumina MiSeq phylogenetic amplicon sequencing shows a large reduction of an uncharacterised succinivibrionaceae and an increase of the methanobrevibacter gottschalkii clade in feed restricted cattle. PLoS ONE. 2015;10:e0133234.
84. Miller TL, Lin C. Description of Methanobrevibacter gottschalkii sp. Nov., Methanobrevibacter thaueri sp. nov., Methanobrevibacter woesei sp. nov. and Methanobrevibacter wolinii sp. nov. Int J Syst Evol Microbiol. 2002;52:819–22.
85. Gilroy R, et al. Extensive microbial diversity within the chicken gut microbiome revealed by metagenomics and culture. PeerJ. 2021;9:e10941.
86. Bowerman KL, et al. Effects of laboratory domestication on the rodent gut microbiome. ISME Commun. 2021;1:1–14.
87. Beresford-Jones BS, et al. The Mouse Gastrointestinal Bacteria Catalogue enables translation between the mouse and human gut microbiotas via functional mapping. Cell Host Microbe. 2022;30:124-138.e8.
88. Zhu J, et al. An expanded gene catalog of mouse gut metagenomes. mSphere. 2021;6:10.
89. Xiao L, et al. A catalog of the mouse gut metagenome. Nat Biotechnol. 2015;33:1103–8.
90. Kieser S, Zdobnov EM, Trajkovski M. Comprehensive mouse microbiota genome catalog reveals major difference to its human counterpart. PLoS Comput Biol. 2022;18:e1009947.
91. Bergamaschi M, et al. Gut microbiome composition differences among breeds impact feed efficiency in swine. Microbiome. 2020;8:110.
92. Massacci FR, et al. Late weaning is associated with increased microbial diversity and Faecalibacterium prausnitzii abundance in the fecal microbiota of piglets. Anim Microbiome. 2020;2:2.
93. de la Cuesta-Zuluaga J, Spector TD, Youngblut ND, Ley RE. Genomic insights into adaptations of trimethylamine-utilizing methanogens to diverse habitats, including the human gut. mSystems. 2021;6:e009390.
94. Mihajlovski A, Doré J, Levenez F, Alric M, Brugère J-F. Molecular evaluation of the human gut methanogenic archaeal microbiota reveals an age-associated increase of the diversity. Environ Microbiol Rep. 2010;2:272–80.
95. Camara A, et al. Clinical evidence of the role of Methanobrevibacter smithii in severe acute malnutrition. Sci Rep. 2021;11:5426.
96. Birgel D, et al. Methanogenesis produces strong 13C enrichment in stromatolites of Lagoa Salgada, Brazil: a modern analogue for Palaeo-/Neoproterozoic stromatolites? Geobiology. 2015;13:245–66.
97. Wang J-X, Xie W, Zhang YG, Meador TB, Zhang CL. Evaluating production of Cyclopentyl Tetraethers by marine group II Euryarchaeota in the Pearl River Estuary and Coastal South China Sea: potential impact on the TEX86 paleothermometer. Front Microbiol. 2017;8:2077.
98. Orsi WD, et al. Climate oscillations reflected within the microbiome of Arabian Sea sediments. Sci Rep. 2017;7:6040.
99. Cavalazzi B, et al. Cellular remains in a ~3.42-billion-year-old subseafloor hydrothermal environment. Sci Adv. 2021;7:3963.
100. More KD, et al. Subseafloor Archaea reflect 139 kyrs of paleodepositional changes in the northern Red Sea. Geobiology. 2021;19:162–72.
101. Baxter BK. Great Salt Lake microbiology: a historical perspective. Int Microbiol. 2018;21:79–95.
102. Yang J, et al. Sedimentary archaeal amoA gene abundance reflects historic nutrient level and salinity fluctuations in Qinghai Lake. Tibetan Plateau Sci Rep. 2015;5:18071.
103. Pearson A, et al. Factors controlling the distribution of archaeal tetraethers in terrestrial hot springs. Appl Environ Microbiol. 2008;74:3523–32.
104. Neubeck A, et al. Microbial community structure in a serpentine-hosted abiotic gas seepage at the chimaera ophiolite, Turkey. Appl Environ Microbiol. 2017;83:e03430.
105. Weyrich LS, et al. Neanderthal behaviour, diet, and disease inferred from ancient DNA in dental calculus. Nature. 2017;544:357–61.
106. KEGG PATHWAY: Methane metabolism + Reference pathway. https://www.genome.jp/pathway/map00680.
107. Kaster A-K, Moll J, Parey K, Thauer RK. Coupling of ferredoxin and heterodisulfide reduction via electron bifurcation in hydrogenotrophic methanogenic archaea. Proc Natl Acad Sci U S A. 2011;108:2981–6.
108. Yan Z, Ferry JG. Electron bifurcation and confurcation in Methanogenesis and Reverse Methanogenesis. Front Microbiol. 2018;9:1322.
109. Berg IA, et al. Autotrophic carbon fixation in archaea. Nat Rev Microbiol. 2010;8:447–60.
110. KEGG MODULE: M00567. https://www.genome.jp/module/M00567.
111. Goldman AD, Leigh JA, Samudrala R. Comprehensive computational analysis of Hmd enzymes and paralogs in methanogenic Archaea. BMC Evol Biol. 2009;9:199.
112. Gottschalk G, Thauer RK. The Na+-translocating methyltransferase complex from methanogenic archaea. Biochim Biophys Acta. 2001;1505:28–36.
113. Thauer RK, Kaster A-K, Seedorf H, Buckel W, Hedderich R. Methanogenic archaea: ecologically relevant differences in energy conservation. Nat Rev Microbiol. 2008;6:579–91.
114. Söllinger A, Urich T. Methylotrophic methanogens everywhere — physiology and ecology of novel players in global methane cycling. Biochem Soc Trans. 2019;47:1895–907.
115. Muñoz-Tamayo R, et al. Hydrogenotrophic methanogens of the mammalian gut: Functionally similar, thermodynamically different-a modelling approach. PLoS ONE. 2019;14:e0226243.
116. Dong M, et al. In vitro methanol production from methyl coenzyme M using the Methanosarcina barkeri MtaABC protein complex. Biotechnol Prog. 2017;33:1243–9.
117. Hoeppner A, et al. Structure of the corrinoid:coenzyme M methyltransferase MtaA from Methanosarcina mazei. Acta Crystallogr D Biol Crystallogr. 2012;68:1549–57.
118. Muñoz-Velasco I, et al. Methanogenesis on early stages of life: ancient but not primordial. Orig Life Evol Biosph. 2018;48:407–20.
119. Hinderberger D, et al. Coordination and binding geometry of methyl-coenzyme M in the red1m state of methyl-coenzyme M reductase. J Biol Inorg Chem. 2008;13:1275–89.
120. Zhang J-W, et al. Newly discovered Asgard archaea Hermodarchaeota potentially degrade alkanes and aromatics via alkyl/benzyl-succinate synthase and benzoyl-CoA pathway. ISME J. 2021;15:1826–43.
121. Lang K, et al. New mode of energy metabolism in the seventh order of methanogens as revealed by comparative genome analysis of "Candidatus methanoplasma termitum." Appl Environ Microbiol. 2015;81:1338–52.
122. Zhang C-J, Pan J, Liu Y, Duan C-H, Li M. Genomic and transcriptomic insights into methanogenesis potential of novel methanogens from mangrove sediments. Microbiome. 2020;8:94.
123. Evans PN, et al. An evolving view of methane metabolism in the Archaea. Nat Rev Microbiol. 2019;17:219–32.
124. MetaCyc EC 6.2.1.1. https://biocyc.org/META/NEW-IMAGE?type=REACTION&object=ACETATE--COA-LIGASE-RXN.
125. Grossart H-P, Frindte K, Dziallas C, Eckert W, Tang KW. Microbial methane production in oxygenated water column of an oligotrophic lake. Proc Natl Acad Sci U S A. 2011;108:19657–61.
126. Lavergne C, et al. Temperature differently affected methanogenic pathways and microbial communities in sub-Antarctic freshwater ecosystems. Environ Int. 2021;154:106575.
127. Kotsyurbenko OR, et al. Acetoclastic and hydrogenotrophic methane production and methanogenic populations in an acidic West-Siberian peat bog. Environ Microbiol. 2004;6:1159–73.
128. Martínez-Álvaro M, et al. Identification of complex rumen microbiome interaction within diverse functional niches as mechanisms affecting the variation of methane emissions in Bovine. Front Microbiol. 2020;11:659.

129. Ferry JG. Fundamentals of methanogenic pathways that are key to the biomethanation of complex biomass. Curr Opin Biotechnol. 2011;22:351–7.
130. Mand TD, Metcalf WW. Energy conservation and hydrogenase function in Methanogenic Archaea, in particular the genus Methanosarcina. Microbiol Mol Biol Rev. 2019;83:10.
131. Fernandes J, et al. Age, dietary fiber, breath methane, and fecal short chain fatty acids are interrelated in Archaea-positive humans. J Nutr. 2013;143:1269–75.
132. Hoedt EC, et al. Culture- and metagenomics-enabled analyses of the Methanosphaera genus reveals their monophyletic origin and differentiation according to genome size. ISME J. 2018;12:2942–53.
133. Tajima K, Aminov R. Structure and function of a nonruminant gut: a porcine model. In: Puniya AK, Singh R, Kamra DN, editors. Rumen microbiology: from evolution to revolution. Springer India; 2015. p. 47–75.
134. Hoedt EC, et al. Differences down-under: alcohol-fueled methanogenesis by archaea present in Australian macropodids. ISME J. 2016;10:2376–88.
135. Meziti A, et al. The reliability of metagenome-assembled genomes (MAGs) in representing natural populations: insights from comparing mags against isolate genomes derived from the same Fecal sample. Appl Environ Microbiol. 2021;87:e02593.
136. Feehan, B. *et al.* Stability and volatility shape the gut bacteriome and mycobiome dynamics in a pig model. *bioRxiv* (2022). https://doi.org/10.1101/2022.02.02.478893.
137. Eren AM, et al. Community-led, integrated, reproducible multi-omics with anvi'o. Nat Microbiol. 2021;6:3–6.
138. Shaiber A, et al. Functional and genetic markers of niche partitioning among enigmatic members of the human oral microbiome. Genome Biol. 2020;21:292.
139. Mölder F, et al. Sustainable data analysis with Snakemake. F1000Res. 2021;10:33.
140. Minoche AE, Dohm JC, Himmelbauer H. Evaluation of genomic high-throughput sequencing data generated on Illumina HiSeq and genome analyzer systems. Genome Biol. 2011;12:R112.
141. Li D, Liu C-M, Luo R, Sadakane K, Lam T-W. MEGAHIT: an ultra-fast single-node solution for large and complex metagenomics assembly via succinct de Bruijn graph. Bioinf. 2015;31:1674–6.
142. Hyatt D, et al. Prodigal: prokaryotic gene recognition and translation initiation site identification. BMC Bioinf. 2010;11:119.
143. Parks DH, et al. A standardized bacterial taxonomy based on genome phylogeny substantially revises the tree of life. Nat Biotechnol. 2018;36:996–1004.
144. Oren A, et al. Proposal to include the rank of phylum in the international code of nomenclature of prokaryotes. Int J Syst Evol Microbiol. 2015;65:4284–7.
145. hmm-source [artifact]. *Anvi'o Home* https://anvio.org/help/7/artifacts/hmm-source/.
146. HMMER. http://hmmer.org/.
147. COG - NCBI. https://www.ncbi.nlm.nih.gov/research/cog.
148. Kanehisa M, Goto S. KEGG: kyoto encyclopedia of genes and genomes. Nucleic Acids Res. 2000;28:27–30.
149. Langmead B, Salzberg SL. Fast gapped-read alignment with Bowtie 2. Nat Methods. 2012;9:357–9.
150. Langmead B, Wilks C, Antonescu V, Charles R. Scaling read aligners to hundreds of threads on general-purpose processors. Bioinformatics. 2019;35:421–32.
151. Danecek P, et al. Twelve years of SAMtools and BCFtools. Gigascience. 2021;10:8.
152. Alneberg J, et al. Binning metagenomic contigs by coverage and composition. Nat Methods. 2014;11:1144–6.
153. Alneberg J, et al. CONCOCT: clustering contigs on coverage and composition. *arXiv [q-bio.GN]* (2013).
154. Murat Eren A, et al. Anvi'o: an advanced analysis and visualization platform for 'omics data. PeerJ. 2015;3:e1319.
155. Pritchard L, Glover RH, Humphris S, Elphinstone JG, Toth IK. Genomics and taxonomy in diagnostics for food security: soft-rotting enterobacterial plant pathogens. Anal Methods. 2016;8:12–24.
156. Lee M. Anvi'o "views" demystified. Meren Lab https://merenlab.org/2017/05/08/anvio-views/.
157. Quince C, et al. DESMAN: a new tool for de novo extraction of strains from metagenomes. Genome Biol. 2017;18:181.
158. RStudio Team. RStudio: integrated development environment for R. RStudio. https://www.rstudio.com/ (2020).
159. pheatmap function - RDocumentation. https://www.rdocumentation.org/packages/pheatmap/versions/1.0.12/topics/pheatmap.
160. Villanueva RAM, Chen ZJ. ggplot2: elegant graphics for data analysis. Measurement. 2019;17:160–7.
161. Wickham H. Forcats: tools for working with categorical variables (Factors) (2022).
162. Wickham H, François R, Henry L, Müller K. dplyr: a grammar of data manipulation (2022).
163. ggplot2 Based Publication Ready Plots. https://rpkgs.datanovia.com/ggpubr/index.html.
164. Brettin T, et al. RASTtk: a modular and extensible implementation of the RAST algorithm for building custom annotation pipelines and annotating batches of genomes. Sci Rep. 2015;5:8365.
165. Davis JJ, et al. The PATRIC bioinformatics resource center: expanding data and analysis capabilities. Nucleic Acids Res. 2020;48:D606–12.
166. Developers IW. Inkscape. https://inkscape.org/.

Publisher's Note